



Research article

Numerical solution of fractional differential equations with temporal two-point BVPs using reproducing kernel Hilbert space method

Yassamine Chellouf¹, Banan Maayah^{1,*}, Shaher Momani^{1,2}, Ahmad Alawneh¹ and Salam Alnabulsi¹

¹ Department of Mathematics, Faculty of Science, The university of Jordan, Amman 11942, Jordan

² Nonlinear Dynamics Research Center (NDRC), Ajman University, Ajman, UAE

* **Correspondence:** Email: b.maayah@ju.edu.jo; Tel: 00962796590252.

Abstract: In this paper, the reproducing kernel Hilbert space method had been extended to model a numerical solution with two-point temporal boundary conditions for the fractional derivative in the Caputo sense, convergent analysis and error bounds are discussed to verify the theoretical results. Numerical examples are given to illustrate the accuracy and efficiency of the presented approach.

Keywords: reproducing kernel Hilbert space method (RKHSM); fractional differential equations; temporal two-point boundary value problems; numerical method; approximate solution

Mathematics Subject Classification: 34A08, 34B15, 46E22, 65R10

1. Introduction

In recent years, the study of fractional derivatives has been an important topic. It has been used to model many phenomena in numerous fields such as science and engineering. There are many interpretations for fractional derivatives, such as the definition of Caputo [1], the definition of Riemann-Liouville [2], the definition of Grunwald-Letnikov [3], and most recently, Conformable [4], Atangana-Baleanu [5], Wallström [6], Jumarie [7], Klimek [8] and others.

In practice, where quantitative results are needed for given real-world problems, numerically approximate solutions can often be demonstrably better, more reliable, more detailed, efficient and cost-effective than analytical ones for certain fractional structures. A number of studies [9–14] were therefore involved in developing approaches for providing estimated solutions. One of these approaches is the Hilbert space kernel reproduction (RKHS) method used for the first time by S. Zaremba for the harmonic and biharmonic functions at the beginning of the 20th century to find solutions for boundary value problems (BVPs).

The RKHS precede the Dirac delta function in many ways, among which we mention providing an important structure for random distribution of multi-round data and, providing accurate approximation of multi-dimensional general functions and the possibility to pick any point in the integration interval.

The RKHS algorithm has been successfully applied to various fields of numerical analysis, computational mathematics, probability and statistics [15,16], biology [17], quantum mechanics and wave mechanics [18]. Therefore wide range of research works have been directed to its applications in various stochastic categories [19], and defined problems involving operator equations [20], partial differential equations [21,22], integrative equations [23,24], and differential integration equations [24–29]. In addition, many studies have focused in recent years on the use of the RKHS method as a framework for seeking approximate numerical solutions to different problems [30–39].

Moreover, the numerical solution of the different groups of BVP can be found in [40–42]. The two-point BVPs has a strong interest in applied mathematics, this kind of problems arise directly from mathematical models or by turning partial differential equations into ordinary differential equations. As this type of problems does not have an exact solution, many special techniques have been used to solve it, including the shooting method [43–44], the collocation method [45–46], the finite difference method [47,48], and the quasilinearization method [49,50]. The continuous genetic algorithm approach was used to solve these schemes in [51–53].

The present paper is structured as follows: in Section 2, we set out some basic concepts and results from fractional calculus theory. In Section 3, the iterative form of the reproducing kernel algorithm is used to build and measure the solution of the fractional differential method with temporal two points. In Section 4 and 5, the convergence and error estimator are discussed to provide a number of numerical results to demonstrate the efficiency and accuracy of the reproducing kernel Hilbert space method. At last in section 6, a conclusion of the results is made.

2. Preliminaries

In applied mathematics and mathematical analysis, there are several definitions of fractional derivatives, Riemann-Liouville and Caputo are the most popular of all [54]. In this section, we list some of these definitions in addition to reproducing kernel spaces on finite domain $[t_0, t_f]$.

Definition 2.1. [55] Let $n \in \mathbb{R}^+$. The operator $\mathcal{J}_{t_0}^n$ defined on $L_1[t_0, t_f]$ by

$$\mathcal{J}_{t_0}^n f(x) := \frac{1}{\Gamma(n)} \int_{t_0}^x (x - \zeta)^{n-1} f(\zeta) d\zeta,$$

for $t_0 \leq x \leq t_f$, is called the Riemann-Liouville fractional integral operator of order n . For $n = 0$, we set $\mathcal{J}_{t_0}^0 := I$, the identity operator.

Definition 2.2. [55] Let $n \in \mathbb{R}^+$ and $m = [n]$. The operator $\mathcal{D}_{t_0}^n$ defined by

$$\mathcal{D}_{t_0}^n f := \mathcal{D}^m \mathcal{J}_{t_0}^{m-n} f = \frac{1}{\Gamma(m-n)} \left(\frac{d}{dx}\right)^m \int_{t_0}^x (x - \zeta)^{m-n-1} f(\zeta) d\zeta,$$

is called the Riemann-Liouville fractional differential operator of order n . For $n = 0$, we set $\mathcal{D}_{t_0}^0 := I$, the identity operator.

Definition 2.3. [55] Let $\alpha \in \mathbb{R}^+$ and $n - 1 < \alpha < n$. The operator $\mathcal{D}_{*t_0}^\alpha$ defined by

$$\mathcal{D}_{*t_0}^\alpha f(x) = \mathcal{J}_{t_0}^{n-\alpha} \mathcal{D}^n f(x) = \frac{1}{\Gamma(n-\alpha)} \int_{t_0}^x (x - \zeta)^{n-\alpha-1} \left(\frac{d}{d\zeta}\right)^n f(\zeta) d\zeta,$$

for $t_0 \leq x \leq t_f$, is called the Caputo differential operator of order α .

Definition 2.4. [35] Let \mathcal{M} be nonempty set, the function $\mathcal{K} : \mathcal{M} \times \mathcal{M} \rightarrow \mathbb{C}$ is a reproducing kernel of the Hilbert space \mathcal{H} if the following conditions are met:

- (1) $\mathcal{K}(\cdot, t) \in \mathcal{M}, \forall t \in \mathcal{M}$,
- (2) the reproducing property: $\forall t \in \mathcal{M}, \forall z \in \mathcal{H} : \langle z(\cdot), \mathcal{K}(\cdot, t) \rangle = z(t)$.

The second condition means that the value of z at the point t is reproduced by the inner product of z with \mathcal{K} .

Note: The reproducing kernel is unique, symmetric and positive definite.

Definition 2.5. $L^2[t_0, t_f] = \{\vartheta \mid \int_{t_0}^{t_f} \vartheta^2(t) dt < \infty\}$.

Definition 2.6. The space $\mathcal{W}_2^1[t_0, t_f]$ is defined as:

$$\mathcal{W}_2^1[t_0, t_f] = \{\vartheta \mid \vartheta \text{ is absolutely continuous real value function, } \vartheta' \in L^2[t_0, t_f]\}.$$

The inner product and its norm are given by:

$$\begin{cases} \langle \vartheta_1(t), \vartheta_2(t) \rangle_{\mathcal{W}_2^1} &= \vartheta_1(t_0)\vartheta_2(t_0) + \int_{t_0}^{t_f} \vartheta_1'(t)\vartheta_2'(t)dt, \\ \|\vartheta\|_{\mathcal{W}_2^1} &= \sqrt{\langle \vartheta(t), \vartheta(t) \rangle_{\mathcal{W}_2^1}}. \end{cases}$$

Definition 2.7. The space $\mathcal{W}_2^2[t_0, t_f]$ is defined by:

$$\mathcal{W}_2^2[t_0, t_f] = \{\vartheta \mid \vartheta, \vartheta' \text{ are absolutely continuous real value functions, } \vartheta'' \in L^2[t_0, t_f], \vartheta(t_0) = 0\}.$$

The inner product and its norm are given by:

$$\begin{cases} \langle \vartheta_1(t), \vartheta_2(t) \rangle_{\mathcal{W}_2^2} &= \vartheta_1(t_0)\vartheta_2(t_0) + \vartheta_1'(t_0)\vartheta_2'(t_0) + \int_{t_0}^{t_f} \vartheta_1''(t)\vartheta_2''(t)dt, \\ \|\vartheta\|_{\mathcal{W}_2^2} &= \sqrt{\langle \vartheta(t), \vartheta(t) \rangle_{\mathcal{W}_2^2}}. \end{cases}$$

Definition 2.8. $\mathcal{W}_2^3[t_0, t_f] = \{\vartheta \mid \vartheta, \vartheta', \vartheta'' \text{ are absolutely continuous, } \vartheta^{(3)} \in L^2[t_0, t_f], \vartheta(t_0) = 0, \vartheta(t_f) = 0\}$.

The inner product and its norm in $\mathcal{W}_2^3[t_0, t_f]$ are given by:

$$\begin{cases} \langle \vartheta_1(t), \vartheta_2(t) \rangle_{\mathcal{W}_2^3} &= \sum_{i=0}^2 \vartheta_1^{(i)}(t_0)\vartheta_2^{(i)}(t_0) + \int_{t_0}^{t_f} \vartheta_1^{(3)}(t)\vartheta_2^{(3)}(t)dt, \\ \|\vartheta\|_{\mathcal{W}_2^3} &= \sqrt{\langle \vartheta(t), \vartheta(t) \rangle_{\mathcal{W}_2^3}}, \vartheta \in \mathcal{W}_2^3. \end{cases}$$

Remark 2.1. The Hilbert space $\mathcal{W}_2^m[t_0, t_f]$ is called a reproducing kernel if for any fixed $t \in [t_0, t_f]$, $\exists \mathcal{K}_i(s) \in \mathcal{W}_2^m[t_0, t_f]$ such that $\langle \vartheta(s), \mathcal{K}_i(s) \rangle_{\mathcal{W}_2^m} = \vartheta(t)$ for any $\vartheta(s) \in \mathcal{W}_2^m[t_0, t_f]$ and $s \in [t_0, t_f]$.

Remark 2.2.

- (1) In [56], \mathcal{W}_2^1 is RKHS and its reproducing kernel is:

$$\mathcal{K}_1(t, s) = \frac{1}{2\sinh 1} [\cosh(t+s-1) + \cosh|t-s| - 1].$$

- (2) In [57], \mathcal{W}_2^2 is RKHS and its reproducing kernel is:

$$\mathcal{K}_2(s, t) = \frac{1}{6} \begin{cases} t(-t^2 + 3s(2+t)) & t \leq s, \\ s(-s^2 + 3t(2+s)) & t > s. \end{cases}$$

3. Reproducing kernel Hilbert space method (RKHSM)

In this section, we develop an iterative method for constructing and calculating fractional differential equations with a temporal two-point solution. In order to emphasize the idea, we start by considering the general form of the BVP:

$$\begin{cases} \mathcal{D}_{t_0}^\alpha X(t) = \mathcal{F}(t, X(t), Y(t)), \\ \mathcal{D}_{t_0}^\alpha Y(t) = \mathcal{G}(t, X(t), Y(t)), \quad t_0 \leq t \leq t_f, \quad 0 \leq \alpha \leq 1. \end{cases} \quad (3.1)$$

Subject to BC's:

$$X(t_0) = \delta, Y(t_f) = \beta. \quad (3.2)$$

where:

$\delta, \beta \in \mathbb{R}$, and \mathcal{D}^α denotes the Caputo fractional derivative of order α and

$$\begin{cases} X(t) = [x_1(t), x_2(t), \dots, x_m(t)], \\ Y(t) = [y_1(t), y_2(t), \dots, y_l(t)], \end{cases} \quad \text{and} \quad \begin{cases} \delta = [\delta_1(t), \delta_2(t), \dots, \delta_m(t)], & \beta = [\beta_1(t), \beta_2(t), \dots, \beta_l(t)], \\ \mathcal{F} = [f_1(t), f_2(t), \dots, f_m(t)], & \mathcal{G} = [g_1(t), g_2(t), \dots, g_l(t)]. \end{cases}$$

We use the RKHS method to obtain a solution of BVPs (3.1) and (3.2) based on the following methodology:

- To attain a problem with homogenous BC's, we first assume that: $Y(t_0) = \gamma$, (γ arbitrary) and

$$\begin{cases} \mathcal{U}(t) = X(t) - X(t_0), \\ \mathcal{V}(t) = Y(t) - Y(t_0). \end{cases} \quad (3.3)$$

We get:

$$\begin{cases} \mathcal{D}_{t_0}^\alpha \mathcal{U}(t) = \mathcal{D}_{t_0}^\alpha X(t), \\ \mathcal{D}_{t_0}^\alpha \mathcal{V}(t) = \mathcal{D}_{t_0}^\alpha Y(t). \end{cases} \quad (3.4)$$

Subject to:

$$\begin{cases} \mathcal{U}(t_0) = 0, \\ \mathcal{V}(t_0) = Y(t_0) - \gamma = 0. \end{cases} \quad (3.5)$$

- Then, we construct the reproducing kernel space $\mathcal{W}_2^2[t_0, t_f]$ in which each function satisfies the homogeneous boundary conditions of (3.5) using the space $\mathcal{W}_2^1[t_0, t_f]$. Take $\mathcal{K}_i(\tau)$ and $\mathcal{R}_i(\tau)$ to be the reproducing kernel functions of the spaces $\mathcal{W}_2^2[t_0, t_f]$ and $\mathcal{W}_2^1[t_0, t_f]$ respectively.
- Next, we define the invertible bounded linear operator $L : \mathcal{W}_2^2[t_0, t_f] \rightarrow \mathcal{W}_2^1[t_0, t_f]$ such that:

$$\begin{cases} L\mathcal{U}(t) = \mathcal{D}_{t_0}^\alpha \mathcal{U}(t), \\ L\mathcal{V}(t) = \mathcal{D}_{t_0}^\alpha \mathcal{V}(t). \end{cases} \quad (3.6)$$

The BVPs (3.4), (3.5) can therefore be transformed to the following form:

$$\begin{cases} L\mathcal{U}(t) = \mathcal{F}(t, X(t), Y(t)), \\ L\mathcal{V}(t) = \mathcal{G}(t, X(t), Y(t)), \\ \mathcal{U}(t_0) = 0, \\ \mathcal{V}(t_0) = 0. \end{cases} \quad (3.7)$$

Where $\mathcal{U}(t)$ and $\mathcal{V}(t)$ are in $\mathcal{W}_2^2[t_0, t_f]$ and $\mathcal{F}, \mathcal{G} \in \mathcal{W}_2^1[t_0, t_f]$.

Applying Riemann-Liouville fractional integral operator $\mathcal{J}_{t_0}^\alpha$ to both sides using $\mathcal{U}(t_0) = 0$ and $\mathcal{V}(t_0) = 0$, we get:

$$\begin{aligned}\mathcal{U}(t) &= \frac{1}{\Gamma(\alpha)} \int_{t_0}^t (t-\tau)^{\alpha-1} \mathcal{F}(\tau, X(\tau), Y(\tau)) d\tau = F(t, X(t), Y(t)), \\ \mathcal{V}(t) &= \frac{1}{\Gamma(\alpha)} \int_{t_0}^t (t-\tau)^{\alpha-1} \mathcal{G}(\tau, X(\tau), Y(\tau)) d\tau = G(t, X(t), Y(t)).\end{aligned}$$

Thus, we can notice that: $L\mathcal{U}(t) = \mathcal{U}(t)$, and so the BVPs are transformed to the equivalent form:

$$\begin{cases} \mathcal{U}(t) = F(t, X(t), Y(t)), \\ \mathcal{V}(t) = G(t, X(t), Y(t)), \\ \mathcal{U}(t_0) = 0, \\ \mathcal{V}(t_0) = 0. \end{cases} \quad (3.8)$$

- When choosing a countable dense set $\{t_i\}_{i=1}^\infty$ from $[t_0, t_f]$ for the reproducing kernel of the space $\mathcal{W}_2^2[t_0, t_f]$, we define a complete system on $\mathcal{W}_2^2[t_0, t_f]$ as: $\Psi_i(t) = L^* \Phi_i(t)$ where $\Phi_i(t) = \mathcal{R}_i(\tau)$, and L^* is the adjoint operator of L .

Lemma 3.1. $\Psi_i(t)$ can be written on the following form:

$$\Psi_i(t) = L_\tau \mathcal{K}_i(\tau)|_{\tau=t_i}.$$

Proof. It is clear that:

$$\begin{aligned}\Psi_i(t) &= L^* \Phi_i(t) = \langle L^* \Phi_i(\tau), \mathcal{K}_i(\tau) \rangle_{\mathcal{W}_2^2}, \\ &= \langle \Phi_i(\tau), L \mathcal{K}_i(\tau) \rangle_{\mathcal{W}_2^1} = L_\tau \mathcal{K}_i|_{\tau=t_i}.\end{aligned}$$

- The orthonormal function system $\{\bar{\Psi}_i^\eta(t)\}_{i=1}^\infty$, $\eta = 1, 2$ of the space $\mathcal{W}_2^2[t_0, t_f]$ can be derived from Gram-Schmidt orthogonalization process of $\{\Psi_i^\eta(t)\}_{i=1}^\infty$ as follows:

$$\bar{\Psi}_i^\eta(t) = \sum_{k=1}^i \mathcal{B}_{ik}^\eta \Psi_k^\eta(t), \quad i = 1, 2, \dots, \quad \eta = 1, 2,$$

where \mathcal{B}_{ik}^η are positive orthogonalization coefficients such that:

$$\mathcal{B}_{11}^\eta = \frac{1}{\|\Psi_1^\eta\|}, \quad \mathcal{B}_{ii}^\eta = \frac{1}{\sqrt{\|\Psi_i^\eta\|^2 - \sum_{k=1}^{i-1} (\mathcal{C}_{ik}^\eta)^2}}, \quad \mathcal{B}_{ij}^\eta = \frac{-\sum_{k=1}^{i-1} \mathcal{C}_{ik}^\eta \mathcal{B}_{kj}^\eta}{\sqrt{\|\Psi_i^\eta\|^2 - \sum_{k=1}^{i-1} (\mathcal{C}_{ik}^\eta)^2}}, \quad j < i. \quad (3.9)$$

\mathcal{C}_{ik}^η given by: $\langle \Psi_i^\eta, \Psi_k^\eta \rangle_{\mathcal{W}_2^2}$.

Theorem 3.1. If the operator L is invertible i.e: L^{-1} exist, and if $\{t_i\}_{i=1}^\infty$ is dense on $[t_0, t_f]$, then $\{\Psi_i^\eta\}_{i=1}^\infty$, $\eta = 1, 2$ is the complete function system of the space $\mathcal{W}_2^2[t_0, t_f]$.

Proof. For each fixed $\mathcal{U}(t)$, $\mathcal{V}(t) \in \mathcal{W}_2^2[t_0, t_f]$, let $\langle \mathcal{U}(t), \Psi_i^1(t) \rangle = 0$, and $\langle \mathcal{V}(t), \Psi_i^2(t) \rangle = 0$, $i = 1, 2, \dots$ that is:

$$\begin{aligned}\langle \mathcal{U}(t), \Psi_i^1(t) \rangle_{\mathcal{W}_2^2} &= \langle \mathcal{U}(t), L^* \Phi_i^1(\tau) \rangle_{\mathcal{W}_2^2} = \langle L\mathcal{U}(t), \Phi_i^1(t) \rangle_{\mathcal{W}_2^1} = L\mathcal{U}(t_i) = 0, \\ \langle \mathcal{V}(t), \Psi_i^2(t) \rangle_{\mathcal{W}_2^2} &= \langle \mathcal{V}(t), L^* \Phi_i^2(\tau) \rangle_{\mathcal{W}_2^2} = \langle L\mathcal{V}(t), \Phi_i^2(t) \rangle_{\mathcal{W}_2^1} = L\mathcal{V}(t_i) = 0,\end{aligned}$$

since $\{t_i\}_{i=1}^{\infty}$ is dense on $[t_0, t_f]$ then $L\mathcal{U}(t) = 0$, and $L\mathcal{V}(t) = 0$ it follows that $\mathcal{U}(t) = 0$, $\mathcal{V}(t) = 0$ since L^{-1} exist and $\mathcal{U}(t)$, $\mathcal{V}(t)$ are continuous.

Theorem 3.2. For each $\mathcal{U}(t)$, $\mathcal{V}(t) \in \mathcal{W}_2^2[t_0, t_f]$ the series

$$\begin{cases} \sum_{i=0}^{\infty} \left\langle \mathcal{U}(t), \bar{\Psi}_i^1(t) \right\rangle_{\mathcal{W}_2^2} \bar{\Psi}_i^1(t), \\ \sum_{i=0}^{\infty} \left\langle \mathcal{V}(t), \bar{\Psi}_i^2(t) \right\rangle_{\mathcal{W}_2^2} \bar{\Psi}_i^2(t), \end{cases}$$

are convergent in the sense of the norm of $\mathcal{W}_2^2[t_0, t_f]$. In contrast if $\{t_i\}_{i=1}^{\infty}$ is dense subset on $[t_0, t_f]$ then the solutions of (3.8) given by:

$$\begin{cases} \mathcal{U}(t) = \sum_{i=1}^{\infty} \sum_{k=1}^i \mathcal{B}_{ik}^1 F(t_k, \mathcal{U}(t_k), \mathcal{V}(t_k)) \bar{\Psi}_i^1(t), \\ \mathcal{V}(t) = \sum_{i=1}^{\infty} \sum_{k=1}^i \mathcal{B}_{ik}^2 G(t_k, \mathcal{U}(t_k), \mathcal{V}(t_k)) \bar{\Psi}_i^2(t). \end{cases} \quad (3.10)$$

Proof. Let $\mathcal{U}(t)$, $\mathcal{V}(t) \in \mathcal{W}_2^2[t_0, t_f]$ be the solutions of (3.8), since $\mathcal{U}(t)$, $\mathcal{V}(t) \in \mathcal{W}_2^2[t_0, t_f]$, and $\sum_{i=1}^{\infty} \left\langle \mathcal{U}(t), \bar{\Psi}_i^1(t) \right\rangle_{\mathcal{W}_2^2[t_0, t_f]} \bar{\Psi}_i^1(t)$ and $\sum_{i=1}^{\infty} \left\langle \mathcal{V}(t), \bar{\Psi}_i^2(t) \right\rangle_{\mathcal{W}_2^2[t_0, t_f]} \bar{\Psi}_i^2(t)$ represent the Fourier series expansion about normal orthogonal system $\{\bar{\Psi}_i^{\eta}(t)\}_{i=1}^{\infty}$, $\eta = 1, 2$, and $\mathcal{W}_2^2[t_0, t_f]$ is Hilbert space, then the series $\sum_{i=1}^{\infty} \left\langle \mathcal{U}(t), \bar{\Psi}_i^1(t) \right\rangle_{\mathcal{W}_2^2[t_0, t_f]} \bar{\Psi}_i^1(t)$, $\sum_{i=1}^{\infty} \left\langle \mathcal{V}(t), \bar{\Psi}_i^2(t) \right\rangle_{\mathcal{W}_2^2[t_0, t_f]} \bar{\Psi}_i^2(t)$ are convergent in the sense of $\|\cdot\|_{\mathcal{W}_2^2[t_0, t_f]}$. In contrast, according to the orthogonal basis $\{\bar{\Psi}_i^{\eta}(t)\}_{i=1}^{\infty}$, we have:

$$\begin{aligned} \mathcal{U}(t) &= \sum_{i=1}^{\infty} \left\langle \mathcal{U}(t), \bar{\Psi}_i^1(t) \right\rangle_{\mathcal{W}_2^2} \bar{\Psi}_i^1(t), \\ &= \sum_{i=1}^{\infty} \left\langle \mathcal{U}(t), \sum_{k=1}^i \mathcal{B}_{ik}^1 \Psi_k^1(t) \right\rangle_{\mathcal{W}_2^2} \bar{\Psi}_i^1(t), \\ &= \sum_{i=1}^{\infty} \sum_{k=1}^i \mathcal{B}_{ik}^1 \left\langle \mathcal{U}(t), \Psi_k^1(t) \right\rangle_{\mathcal{W}_2^2} \bar{\Psi}_i^1(t), \\ &= \sum_{i=1}^{\infty} \sum_{k=1}^i \mathcal{B}_{ik}^1 \left\langle \mathcal{U}(t), L^* \Phi_k^1(t) \right\rangle_{\mathcal{W}_2^2} \bar{\Psi}_i^1(t), \\ &= \sum_{i=1}^{\infty} \sum_{k=1}^i \mathcal{B}_{ik}^1 \left\langle L\mathcal{U}(t), \Phi_k^1(t) \right\rangle_{\mathcal{W}_2^1} \bar{\Psi}_i^1(t), \\ &= \sum_{i=1}^{\infty} \sum_{k=1}^i \mathcal{B}_{ik}^1 \left\langle F(t_k, \mathcal{U}(t_k), \mathcal{V}(t_k)), \Phi_k^1(t) \right\rangle_{\mathcal{W}_2^1} \bar{\Psi}_i^1(t), \\ &= \sum_{i=1}^{\infty} \sum_{k=1}^i \mathcal{B}_{ik}^1 F(t_k, \mathcal{U}(t_k), \mathcal{V}(t_k)) \bar{\Psi}_i^1(t). \end{aligned}$$

The same for finding $\mathcal{V}(t)$:

$$\mathcal{V}(t) = \sum_{i=1}^{\infty} \sum_{k=1}^i \mathcal{B}_{ik}^2 G(t_k, \mathcal{U}(t_k), \mathcal{V}(t_k)) \bar{\Psi}_i^2(t).$$

The theorem is proved.

Since \mathcal{W}_2^2 is Hilbert space we get:

$$\sum_{i=1}^{\infty} \sum_{k=1}^i \mathcal{B}_{ik}^1 \left\langle L\mathcal{U}(t), \Phi_k^1(t) \right\rangle_{\mathcal{W}_2^1} \bar{\Psi}_i^1(t) < \infty \text{ and } \sum_{i=1}^{\infty} \sum_{k=1}^i \mathcal{B}_{ik}^2 \left\langle L\mathcal{V}(t), \Phi_k^2(t) \right\rangle_{\mathcal{W}_2^1} \bar{\Psi}_i^2(t) < \infty.$$

Hence:

$$\begin{cases} \mathcal{U}_n(t) = \sum_{i=1}^n \sum_{k=1}^i \mathcal{B}_{ik}^1 F(t_k, \mathcal{U}(t_k), \mathcal{V}(t_k)) \bar{\Psi}_i^1(t), \\ \mathcal{V}_n(t) = \sum_{i=1}^n \sum_{k=1}^i \mathcal{B}_{ik}^2 G(t_k, \mathcal{U}(t_k), \mathcal{V}(t_k)) \bar{\Psi}_i^2(t), \end{cases} \quad (3.11)$$

are convergent in the sense of $\|\cdot\|_{\mathcal{W}_2^2}$ and (3.11) represents the numerical solution of (3.8).

Remark 3.1.

- (1) If the system (3.7) is linear, then the exact solutions can be found directly from (3.10).
 (2) If the system (3.7) is non linear, then the exact and numerical solutions can be obtained by:

$$\begin{cases} \mathcal{U}(t) = \sum_{i=1}^{\infty} \mathcal{A}_i^1 \bar{\Psi}_i^1(t), \\ \mathcal{V}(t) = \sum_{i=1}^{\infty} \mathcal{A}_i^2 \bar{\Psi}_i^2(t), \end{cases} \quad (3.12)$$

where:

$$\begin{cases} \mathcal{A}_i^1 = \sum_{k=1}^i \mathcal{B}_{ik}^1 F(t_k, \mathcal{U}_{k-1}(t_k), \mathcal{V}_{k-1}(t_k)), \\ \mathcal{A}_i^2 = \sum_{k=1}^i \mathcal{B}_{ik}^2 G(t_k, \mathcal{U}_{k-1}(t_k), \mathcal{V}_{k-1}(t_k)). \end{cases} \quad (3.13)$$

We use the known quantities λ_i^η , $\eta = 1, 2$ to approximate the unknowns \mathcal{A}_i^η , $\eta = 1, 2$ as follows: we put $t_1 = t_0$ and set $\mathcal{U}_0(t_1) = \mathcal{U}(t_1)$, $\mathcal{V}_0(t_1) = \mathcal{V}(t_1)$ then $\mathcal{U}_0(t_1) = \mathcal{V}_0(t_1) = 0$ from the conditions of (3.8), and define the n -term approximation to $\mathcal{U}(t)$, $\mathcal{V}(t)$ by:

$$\begin{cases} \mathcal{U}_n(t) = \sum_{i=1}^n \lambda_i^1 \bar{\Psi}_i^1(t), \\ \mathcal{V}_n(t) = \sum_{i=1}^n \lambda_i^2 \bar{\Psi}_i^2(t), \end{cases} \quad (3.14)$$

where the coefficient λ_i^η ($\eta = 1, 2$, $i = 1, 2, \dots, n$), are presented as follows:

$$\begin{cases} \lambda_n^1 = \sum_{k=1}^n \mathcal{B}_{ik}^1 F(t_k, \mathcal{U}_{k-1}(t_k), \mathcal{V}_{k-1}(t_k)), \\ \lambda_n^2 = \sum_{k=1}^n \mathcal{B}_{ik}^2 G(t_k, \mathcal{U}_{k-1}(t_k), \mathcal{V}_{k-1}(t_k)), \end{cases} \quad (3.15)$$

and so:

$$\begin{cases} \mathcal{U}_n(t) = \sum_{i=1}^n \lambda_i^1 \bar{\Psi}_i^1(t), \\ \mathcal{V}_n(t) = \sum_{i=1}^n \lambda_i^2 \bar{\Psi}_i^2(t). \end{cases} \quad (3.16)$$

We can guarantee that the approximations $\mathcal{U}_n(t)$, $\mathcal{V}_n(t)$ satisfies the conditions enjoined by (3.7) through the iterative process of (3.16).

4. Error estimation and convergence

In this section, we present some convergence theories to emphasize that the approximate solution we got is close to the exact solution. Indeed, this finding is very powerful and efficient to RKHS theory and its applications.

Lemma 4.1. $\|\mathcal{U}_n(t)\|_{\mathcal{W}_2}^\infty$, and $\|\mathcal{V}_n(t)\|_{\mathcal{W}_2}^\infty$ are monotone increasing in the sense of the norm of $\|\cdot\|_{\mathcal{W}_2}^2$.

Proof. Since $\|\bar{\Psi}_i^\eta(t)\|_{i=1}^\infty$, $\eta = 1, 2$ are the complete orthonormal systems in the space $\mathcal{W}_2^2[t_0, t_f]$ then we have:

$$\begin{cases} \|\mathcal{U}_n(t)\|_{\mathcal{W}_2}^2 = \langle \mathcal{U}_n(t), \mathcal{U}_n(t) \rangle_{\mathcal{W}_2} = \left\langle \sum_{i=1}^n \lambda_i^1 \bar{\Psi}_i^1(t), \sum_{i=1}^n \lambda_i^1 \bar{\Psi}_i^1(t) \right\rangle_{\mathcal{W}_2} = \sum_{i=1}^n (\lambda_i^1)^2, \\ \|\mathcal{V}_n(t)\|_{\mathcal{W}_2}^2 = \langle \mathcal{V}_n(t), \mathcal{V}_n(t) \rangle_{\mathcal{W}_2} = \left\langle \sum_{i=1}^n \lambda_i^2 \bar{\Psi}_i^2(t), \sum_{i=1}^n \lambda_i^2 \bar{\Psi}_i^2(t) \right\rangle_{\mathcal{W}_2} = \sum_{i=1}^n (\lambda_i^2)^2. \end{cases}$$

Thus $\|\mathcal{U}_n(t)\|_{\mathcal{W}_2}$, $\|\mathcal{V}_n(t)\|_{\mathcal{W}_2}$ are monotone increasing.

Lemma 4.2. As $n \rightarrow \infty$, the approximate solutions $\mathcal{U}_n(t)$, $\mathcal{V}_n(t)$ and its derivatives $\mathcal{U}'_n(t)$, $\mathcal{V}'_n(t)$ are uniformly convergent to the exact solutions $\mathcal{U}(t)$, $\mathcal{V}(t)$ and its derivatives $\mathcal{U}'(t)$, $\mathcal{V}'(t)$ respectively.

Proof. For any $t \in [t_0, t_f]$:

$$\begin{aligned} |\mathcal{U}'_n(t) - \mathcal{U}'(t)| &= \left| \langle \mathcal{U}_n(t) - \mathcal{U}(t), \mathcal{K}'_t(\tau) \rangle_{\mathcal{W}_2^2} \right|, \\ &\leq \|\mathcal{K}'_t(\tau)\|_{\mathcal{W}_2^2} \|\mathcal{U}_n(t) - \mathcal{U}(t)\|_{\mathcal{W}_2^2}, \\ &\leq \mathcal{N}_1 \|\mathcal{U}_n(t) - \mathcal{U}(t)\|_{\mathcal{W}_2^2}, \quad \mathcal{N}_1 \in \mathbb{R}, \end{aligned}$$

and

$$|\mathcal{V}'_n(t) - \mathcal{V}'(t)| \leq \mathcal{N}_2 \|\mathcal{V}_n(t) - \mathcal{V}(t)\|_{\mathcal{W}_2^2}, \quad \mathcal{N}_2 \in \mathbb{R},$$

if $\|\mathcal{U}_n(t) - \mathcal{U}(t)\|_{\mathcal{W}_2^2} \rightarrow 0$, $\|\mathcal{V}_n(t) - \mathcal{V}(t)\|_{\mathcal{W}_2^2} \rightarrow 0$ as $n \rightarrow \infty$, then the approximate solutions $\mathcal{U}_n^{(i)}(t)$, $\mathcal{V}_n^{(i)}(t)$ are uniformly converges to the exact solutions $\mathcal{U}^{(i)}(t)$, $\mathcal{V}^{(i)}(t)$ $i = 1, 2$ respectively.

Theorem 4.1. If

$$\begin{cases} \mathcal{U}_n(t) \rightarrow \mathcal{U}(t), \\ \mathcal{V}_n(t) \rightarrow \mathcal{V}(t), \end{cases}$$

and $F(t, \mathcal{U}(t), \mathcal{V}(t))$, $G(t, \mathcal{U}(t), \mathcal{V}(t))$ are continuous in $[t_0, t_f]$, then:

$$\begin{cases} F(t_n, \mathcal{U}_{n-1}(t_n), \mathcal{V}_{n-1}(t_n)) \rightarrow F(t, \mathcal{U}(t), \mathcal{V}(t)) \\ G(t_n, \mathcal{U}_{n-1}(t_n), \mathcal{V}_{n-1}(t_n)) \rightarrow G(t, \mathcal{U}(t), \mathcal{V}(t)) \end{cases} \quad \text{as } n \rightarrow \infty. \quad (4.1)$$

Proof. For the first part, we will prove that:

$$\begin{cases} \mathcal{U}_{n-1}(t_n) \rightarrow \mathcal{U}(t), \\ \mathcal{V}_{n-1}(t_n) \rightarrow \mathcal{V}(t), \end{cases}$$

it is easy to see that:

$$\begin{cases} |\mathcal{U}_{n-1}(t_n) - \mathcal{U}(t)| = |\mathcal{U}_{n-1}(t_n) - \mathcal{U}_{n-1}(t) + \mathcal{U}_{n-1}(t) - \mathcal{U}(t)| \leq |\mathcal{U}_{n-1}(t_n) - \mathcal{U}_{n-1}(t)| + |\mathcal{U}_{n-1}(t) - \mathcal{U}(t)|, \\ |\mathcal{V}_{n-1}(t_n) - \mathcal{V}(t)| = |\mathcal{V}_{n-1}(t_n) - \mathcal{V}_{n-1}(t) + \mathcal{V}_{n-1}(t) - \mathcal{V}(t)| \leq |\mathcal{V}_{n-1}(t_n) - \mathcal{V}_{n-1}(t)| + |\mathcal{V}_{n-1}(t) - \mathcal{V}(t)|, \end{cases}$$

by reproducing property of $\mathcal{K}_i(\tau)$ we have:

$$\begin{cases} \mathcal{U}_{n-1}(t_n) = \langle \mathcal{U}_{n-1}(\tau), \mathcal{K}_n(\tau) \rangle, \\ \mathcal{V}_{n-1}(t_n) = \langle \mathcal{V}_{n-1}(\tau), \mathcal{K}_n(\tau) \rangle, \end{cases}$$

and

$$\begin{cases} \mathcal{U}_{n-1}(t) = \langle \mathcal{U}_{n-1}(\tau), \mathcal{K}_i(\tau) \rangle, \\ \mathcal{V}_{n-1}(t) = \langle \mathcal{V}_{n-1}(\tau), \mathcal{K}_i(\tau) \rangle, \end{cases}$$

thus

$$\begin{cases} |\mathcal{U}_{n-1}(t_n) - \mathcal{U}_{n-1}(t)| = \left| \langle \mathcal{U}_{n-1}(\tau), \mathcal{K}_n(\tau) - \mathcal{K}_i(\tau) \rangle_{\mathcal{W}_2^2} \right| \leq \|\mathcal{U}_{n-1}(\tau)\|_{\mathcal{W}_2^2} \|\mathcal{K}_n(\tau) - \mathcal{K}_i(\tau)\|_{\mathcal{W}_2^2}, \\ |\mathcal{V}_{n-1}(t_n) - \mathcal{V}_{n-1}(t)| = \left| \langle \mathcal{V}_{n-1}(\tau), \mathcal{K}_n(\tau) - \mathcal{K}_i(\tau) \rangle_{\mathcal{W}_2^2} \right| \leq \|\mathcal{V}_{n-1}(\tau)\|_{\mathcal{W}_2^2} \|\mathcal{K}_n(\tau) - \mathcal{K}_i(\tau)\|_{\mathcal{W}_2^2}, \end{cases}$$

and from the symmetric property of $\mathcal{K}_i(\tau)$ we get:

$$\|\mathcal{K}_n(\tau) - \mathcal{K}_i(\tau)\|_{\mathcal{W}_2^2} \xrightarrow{n \rightarrow \infty} 0,$$

hence: $|\mathcal{U}_{n-1}(t_n) - \mathcal{U}_{n-1}(t)| \rightarrow 0$ as $t_n \rightarrow t$.

By lemma (4.2)

$$\begin{cases} \mathcal{U}_n(t) \xrightarrow{c.u} \mathcal{U}(t), \\ \mathcal{V}_n(t) \xrightarrow{c.u} \mathcal{V}(t), \end{cases}$$

thus:

$$\begin{cases} |\mathcal{U}_{n-1}(t) - \mathcal{U}(t)| \rightarrow 0 \\ |\mathcal{V}_{n-1}(t) - \mathcal{V}(t)| \rightarrow 0 \end{cases} \text{ as } n \rightarrow \infty.$$

Therefore

$$\begin{cases} \mathcal{U}_{n-1}(t_n) \rightarrow \mathcal{U}(t), \\ \mathcal{V}_{n-1}(t_n) \rightarrow \mathcal{V}(t), \end{cases}$$

in the sense of the $\|\cdot\|_{\mathcal{W}_2^2}$ as $t_n \rightarrow t$ and $n \rightarrow \infty$ for any $t \in [t_0, t_f]$.

Moreover, since F and G are continuous, we obtain:

$$\begin{cases} F(t_n, \mathcal{U}_{n-1}(t_n), \mathcal{V}_{n-1}(t_n)) \rightarrow F(t, \mathcal{U}(t), \mathcal{V}(t)) \\ G(t_n, \mathcal{U}_{n-1}(t_n), \mathcal{V}_{n-1}(t_n)) \rightarrow G(t, \mathcal{U}(t), \mathcal{V}(t)) \end{cases} \text{ as } n \rightarrow \infty.$$

Theorem 4.2. Suppose that $\|\mathcal{U}_n\|_{\mathcal{W}_2^2}$ and $\|\mathcal{V}_n\|_{\mathcal{W}_2^2}$ are bounded in Eq (3.14), if $\{t_i\}_{i=1}^{\infty}$ is dense on $[t_0, t_f]$, then the approximate solutions $\mathcal{U}_n(t)$, $\mathcal{V}_n(t)$ in Eq (3.14) convergent to the exact solutions $\mathcal{U}(t)$, $\mathcal{V}(t)$ of Eq (3.7) in the space $\mathcal{W}_2^2[t_0, t_f]$ and $\mathcal{U}(t)$, $\mathcal{V}(t)$ given by (3.12).

Proof. We first start by proving the convergence of $\mathcal{U}_n(t)$ and $\mathcal{V}_n(t)$ from Eq (3.14) we conclude that:

$$\begin{cases} \mathcal{U}_{n+1}(t) = \mathcal{U}_n(t) + \lambda_{n+1}^1 \bar{\Psi}_{n+1}^1(t), \\ \mathcal{V}_{n+1}(t) = \mathcal{V}_n(t) + \lambda_{n+1}^2 \bar{\Psi}_{n+1}^2(t), \end{cases}$$

by orthogonality of $\{\bar{\Psi}_i^\eta(t)\}_{i=1}^{\infty}$, $(\eta) = 1, 2$ we get:

$$\begin{cases} \|\mathcal{U}_{n+1}(t)\|_{\mathcal{W}_2^2}^2 = \|\mathcal{U}_n(t)\|_{\mathcal{W}_2^2}^2 + (\lambda_{n+1}^1)^2 = \dots = \|\mathcal{U}_0(t)\|_{\mathcal{W}_2^2}^2 + \sum_{i=1}^{n+1} (\lambda_i^1)^2, \\ \|\mathcal{V}_{n+1}(t)\|_{\mathcal{W}_2^2}^2 = \|\mathcal{V}_n(t)\|_{\mathcal{W}_2^2}^2 + (\lambda_{n+1}^2)^2 = \dots = \|\mathcal{V}_0(t)\|_{\mathcal{W}_2^2}^2 + \sum_{i=1}^{n+1} (\lambda_i^2)^2, \end{cases}$$

$\|\mathcal{U}_n(t)\|_{\mathcal{W}_2^2}$, $\|\mathcal{V}_n(t)\|_{\mathcal{W}_2^2}$ are monotone increasing by Lemma (4.1). From the assumption that $\|\mathcal{U}_n(t)\|_{\mathcal{W}_2^2}$, $\|\mathcal{V}_n(t)\|_{\mathcal{W}_2^2}$ are bounded, $\|\mathcal{U}_n(t)\|_{\mathcal{W}_2^2}$, $\|\mathcal{V}_n(t)\|_{\mathcal{W}_2^2}$ are convergent as $n \rightarrow \infty$, then $\exists c, d$ constants such that

$$\begin{cases} \sum_{i=1}^{\infty} (\lambda_i^1)^2 = c, \\ \sum_{i=1}^{\infty} (\lambda_i^2)^2 = d, \end{cases}$$

if $m > n$ using

$$\begin{cases} (\mathcal{U}_m - \mathcal{U}_{m-1}) \perp (\mathcal{U}_{m-1} - \mathcal{U}_{m-2}) \perp \dots \perp (\mathcal{U}_{n+1} - \mathcal{U}_n), \\ (\mathcal{V}_m - \mathcal{V}_{m-1}) \perp (\mathcal{V}_{m-1} - \mathcal{V}_{m-2}) \perp \dots \perp (\mathcal{V}_{n+1} - \mathcal{V}_n), \end{cases}$$

further that

$$\begin{cases} \|\mathcal{U}_m(t) - \mathcal{U}_{m-1}(t)\|_{\mathcal{W}_2^2}^2 = (\lambda_m^1)^2, \\ \|\mathcal{V}_m(t) - \mathcal{V}_{m-1}(t)\|_{\mathcal{W}_2^2}^2 = (\lambda_m^2)^2, \end{cases}$$

so:

$$\begin{cases} \|\mathcal{U}_m(t) - \mathcal{U}_n(t)\|_{\mathcal{W}_2^2}^2 = \sum_{i=n+1}^m (\lambda_i^1)^2 \longrightarrow 0 \\ \|\mathcal{V}_m(t) - \mathcal{V}_n(t)\|_{\mathcal{W}_2^2}^2 = \sum_{i=n+1}^m (\lambda_i^2)^2 \longrightarrow 0 \end{cases} \text{ as } n, m \rightarrow \infty,$$

since $\mathcal{W}_2^2[t_0, t_f]$ is complete, $\exists \mathcal{U}(t), \mathcal{V}(t)$ in $\mathcal{W}_2^2[t_0, t_f]$ such that

$$\begin{cases} \mathcal{U}_n(t) \longrightarrow \mathcal{U}(t) \\ \mathcal{V}_n(t) \longrightarrow \mathcal{V}(t) \end{cases} \text{ as } n \longrightarrow \infty,$$

in the sense of the norm of $\mathcal{W}_2^2[t_0, t_f]$.

Now, we prove that $\mathcal{U}(t), \mathcal{V}(t)$ are solutions of Eq (3.7). Since $\{t_i\}_{i=1}^\infty$ is dense on $[t_0, t_f], \forall t \in [t_0, t_f], \exists$ subsequence $\{t_{n_j}\}_{j \rightarrow \infty}$ such that $t_{n_j} \longrightarrow t$. From lemma (3) and (4) in [25] we have:

$$\begin{cases} L\mathcal{U}(t_{n_j}) = F(t_{n_j}, \mathcal{U}_{n_j-1}(t_{n_j}), \mathcal{V}_{n_j-1}(t_{n_j})), \\ L\mathcal{V}(t_{n_j}) = G(t_{n_j}, \mathcal{U}_{n_j-1}(t_{n_j}), \mathcal{V}_{n_j-1}(t_{n_j})), \end{cases}$$

let j goes to ∞ , by theorem (4.1) and the continuity of F and G we have:

$$\begin{cases} L\mathcal{U}(t) = F(t, \mathcal{U}(t), \mathcal{V}(t)), \\ L\mathcal{V}(t) = G(t, \mathcal{U}(t), \mathcal{V}(t)), \end{cases}$$

that is $\mathcal{U}(t), \mathcal{V}(t)$ are solutions of Eq (3.7).

Theorem 4.3. Let $\xi_n = \|\mathcal{U}_n(t) - \mathcal{U}(t)\|, \xi'_n = \|\mathcal{V}_n(t) - \mathcal{V}(t)\|$, where: $\mathcal{U}_n(t), \mathcal{V}_n(t), \mathcal{U}(t), \mathcal{V}(t)$ denote the approximate and the exact solutions respectively, then the sequences of numbers $\{\xi_n\}, \{\xi'_n\}$ are decreasing in the sense of the norm $\|\cdot\|_{\mathcal{W}_2^2}$ and $\xi_n \xrightarrow{n \rightarrow \infty} 0, \xi'_n \xrightarrow{n \rightarrow \infty} 0$.

Proof. From the extension form of $\mathcal{U}(t), \mathcal{V}(t)$ and $\mathcal{U}_n(t), \mathcal{V}_n(t)$ in Eqs (3.12), (3.14) and (3.15) we can write:

$$\begin{cases} \|\xi_n\|_{\mathcal{W}_2^2}^2 = \left\| \sum_{i=n+1}^\infty \lambda_i^1 \bar{\Psi}_i^1(t) \right\|_{\mathcal{W}_2^2}^2 = \sum_{i=n+1}^\infty (\lambda_i^1)^2, \\ \|\xi'_n\|_{\mathcal{W}_2^2}^2 = \left\| \sum_{i=n+1}^\infty \lambda_i^2 \bar{\Psi}_i^2(t) \right\|_{\mathcal{W}_2^2}^2 = \sum_{i=n+1}^\infty (\lambda_i^2)^2, \end{cases}$$

and

$$\begin{cases} \|\xi_{n-1}\|_{\mathcal{W}_2^2}^2 = \left\| \sum_{i=n}^\infty \lambda_i^1 \bar{\Psi}_i^1(t) \right\|_{\mathcal{W}_2^2}^2 = \sum_{i=n}^\infty (\lambda_i^1)^2, \\ \|\xi'_{n-1}\|_{\mathcal{W}_2^2}^2 = \left\| \sum_{i=n}^\infty \lambda_i^2 \bar{\Psi}_i^2(t) \right\|_{\mathcal{W}_2^2}^2 = \sum_{i=n}^\infty (\lambda_i^2)^2. \end{cases}$$

Clearly: $\|\xi_n\|_{\mathcal{W}_2^2}, \|\xi'_n\|_{\mathcal{W}_2^2}$ are decreasing in a sense of $\|\cdot\|_{\mathcal{W}_2^2}$ from theorem (3.2) the series $\sum_{i=1}^\infty \lambda_i^1 \bar{\Psi}_i^1(t), \sum_{i=1}^\infty \lambda_i^2 \bar{\Psi}_i^2(t)$ are convergent, thus $\|\xi_n\|_{\mathcal{W}_2^2} \longrightarrow 0, \|\xi'_n\|_{\mathcal{W}_2^2} \longrightarrow 0$ as $n \longrightarrow \infty$.

Theorem 4.4. The approximate solutions $\mathcal{U}_n(t), \mathcal{V}_n(t)$ of (3.7) converge to its exact solutions $\mathcal{U}(t), \mathcal{V}(t)$ with not less than the second order convergence. That is: $\|\mathcal{U}_n - \mathcal{U}\| \leq Mk^2$ and $\|\mathcal{V}_n - \mathcal{V}\| \leq Nk^2$, where $k = \frac{t_f - t_0}{n}$.

Proof. See [36].

5. Numerical examples and algorithm

Numerical examples are conducted in order to verify the accuracy of this method. Computations are performed using Mathematica 11.0.

Algorithm 1: Use the following stages to approximate the solutions of BVPs (3.4) and (3.5) based on RKHS method.

- **Stage A:** Fixed $t \in [t_0, t_f]$ and set $\tau \in [t_0, t_f]$

for $i = 1, \dots, n$ do the following stages:

- **stage 1:** set $t_i = t_0 + \frac{(t_f - t_0)i}{n}$;

- **stage 2:** if $\tau \leq t$ let

$$\mathcal{K}_\tau(t) = \sum_{i=0}^3 p_i(t)\tau^i;$$

else let

$$\mathcal{K}_\tau(t) = \sum_{i=0}^3 q_i(t)\tau^i.$$

- **stage 3:** For $\eta = 1, 2$;

set

$$\Psi_i^\eta(t) = L_\tau \mathcal{K}_i(\tau)|_{\tau=t_i}.$$

Output the orthogonal functions system $\Psi_i^\eta(t)$.

- **Stage B:** Obtain the orthogonalization coefficients \mathcal{B}_{ij}^η as follows:

For $\eta = 1, 2$;

For $i = 1, \dots, n$;

For $j = 1, \dots, i$ set $C_{ik}^\eta = \langle \Psi_i^\eta, \Psi_j^\eta \rangle_{\mathcal{W}_2^\eta}$ and $\mathcal{B}_{11} = \frac{1}{\text{Sqrt}(C_{11}^\eta)}$.

Output C_{ij}^η and \mathcal{B}_{11} .

- **Stage C:** For $\eta = 1, 2$;

For $i = 1, \dots, n$, set $\mathcal{B}_{ii}^\eta = (\|\Psi_i^\eta\|_{\mathcal{W}_2^\eta}^2 - \sum_{k=1}^{i-1} (C_{ik}^\eta)^2)^{\frac{-1}{2}}$;

else if $j \neq i$ set $\mathcal{B}_{ij}^\eta = -(\sum_{k=1}^{i-1} C_{ik}^\eta \mathcal{B}_{kj}^\eta) \cdot (\|\Psi_i^\eta\|_{\mathcal{W}_2^\eta}^2 - \sum_{k=1}^{i-1} (C_{ik}^\eta)^2)^{\frac{-1}{2}}$.

Output the orthogonalization coefficients \mathcal{B}_{ij}^η .

- **Stage D:** For $\eta = 1, 2$;

For $i = 1, \dots, n$ set $\bar{\Psi}_i^\eta(t) = \sum_{k=1}^i \mathcal{B}_{ik}^\eta \Psi_i^\eta(t)$.

Output the orthonormal functions system $\bar{\Psi}_i^\eta(t)$.

- **Stage E:** Set $t_1 = 0$ and choose $\mathcal{U}_0(t_1) = 0$, $\mathcal{V}_0(t_1) = 0$;

For $\eta = 1, 2$;

For $i = 1$ set

$$\begin{cases} \lambda_1^1 = \mathcal{B}_{11}^1 F(t_1, \mathcal{U}_0(t_1), \mathcal{V}_0(t_1)), \\ \lambda_1^2 = \mathcal{B}_{11}^2 G(t_1, \mathcal{U}_0(t_1), \mathcal{V}_0(t_1)), \end{cases} \quad \text{and} \quad \begin{cases} \mathcal{U}_1(t) = \lambda_1^1 \bar{\Psi}_1^1(t), \\ \mathcal{V}_1(t) = \lambda_1^2 \bar{\Psi}_1^2(t). \end{cases}$$

For $i = 2, 3, \dots, n$ set

$$\begin{cases} \lambda_i^1 = \sum_{k=1}^i \mathcal{B}_{nk}^1 F(t_k, \mathcal{U}_{k-1}(t_k), \mathcal{V}_{k-1}(t_k)), \\ \lambda_i^2 = \sum_{k=1}^i \mathcal{B}_{nk}^2 G(t_k, \mathcal{U}_{k-1}(t_k), \mathcal{V}_{k-1}(t_k)), \end{cases}$$

set

$$\begin{cases} \mathcal{U}_n(t) = \sum_{i=1}^n \lambda_i^1 \overline{\Psi}_i^1(t), \\ \mathcal{V}_n(t) = \sum_{i=1}^n \lambda_i^2 \overline{\Psi}_i^2(t). \end{cases}$$

Outcome the numerical solutions $\mathcal{U}_n(t)$, $\mathcal{V}_n(t)$.

Then we implement the above algorithm using numerical simulations. We arrange the resulting data in tables and graphs for examples discussed on $[t_0, t_f]$ as follows:

Example 5.1. Consider the following system:

$$\begin{cases} \mathcal{D}^\alpha \omega(t) = -4\omega + 3\Theta + 6, \\ \mathcal{D}^\alpha \Theta(t) = -2.4\omega + 1.6\Theta + 3.6, \quad 0 \leq t \leq 0.5, \quad 0 \leq \alpha \leq 1, \end{cases}$$

subject to:

$$\begin{cases} \omega(0) = 0, \\ \Theta(0.5) = -2.25e^{-1} + 2.25e^{-0.2}, \end{cases}$$

with exact solution when $\alpha = 1$ is:

$$\begin{cases} \omega(t) = -3.375e^{-2t} + 1.875e^{-0.4t} + 1.5, \\ \Theta(t) = -2.25e^{-2t} + 2.25e^{-0.4t}. \end{cases}$$

After the initial conditions have been homogenised and algorithm 1 used, apply $t_i = \frac{0.5i}{n}$, $i = 1, n$ and $n = 40$, the tables 1 and 2 describe the exact solutions of $\omega(t)$ and $\Theta(t)$ and approximate solutions for different values of α .

Table 1. Numerical results for $\omega(t)$ of example 5.1.

t	Exact Sol of $\omega(t)$	App Sol of $\omega(t)$	$\alpha = 0.9$	$\alpha = 0.8$	$\alpha = 0.7$	Abs Error	Rel Error
0.	0.	0.	0.	0.	0.	0.	Indeterminate
0.1	0.538264	0.538235	0.672451	0.820896	0.975714	2.8979×10^{-5}	5.3838×10^{-5}
0.2	0.968513	0.968496	1.10364	1.22992	1.34045	1.6912×10^{-5}	1.7462×10^{-5}
0.3	1.31074	1.31073	1.41427	1.49734	1.55882	7.6470×10^{-6}	5.8341×10^{-6}
0.4	1.58128	1.58128	1.64374	1.68334	1.70372	5.4565×10^{-7}	3.4507×10^{-7}
0.5	1.79353	1.79353	1.81496	1.8167	1.805	4.8467×10^{-6}	2.7023×10^{-6}

Table 2. Numerical results for $\Theta(t)$ of example 5.1.

t	Exact Sol $\Theta(t)$	App Sol of $\Theta(t)$	$\alpha = 0.9$	$\alpha = 0.8$	$\alpha = 0.7$	Abs Error	Rel Error
0.	0.	0.	0.	0.	0.	0.	Complex Infinity
0.1	0.319632	0.31963	0.397424	0.48192	0.56754	1.7129×10^{-6}	5.3589×10^{-6}
0.2	0.568792	0.568797	0.643125	0.70952	0.76353	5.6398×10^{-6}	9.9154×10^{-6}
0.3	0.760745	0.760756	0.812467	0.84948	0.87141	1.1152×10^{-5}	1.4659×10^{-5}
0.4	0.906333	0.906349	0.930619	0.93950	0.93585	1.5248×10^{-5}	1.6823×10^{-5}
0.5	1.01442	1.01443	1.01229	0.99765	0.97506	1.8229×10^{-5}	1.7970×10^{-5}

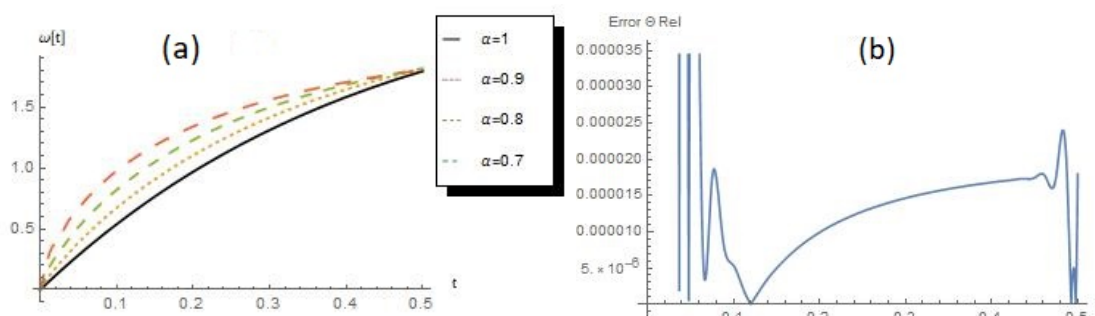


Figure 1. Solution and graphical curves of Example 5.1.

Graphs of the approximate solutions of $\omega(t)$ are plotted in Figure 1 (a), for different values of α . It is obvious from Figure 1 (a) that the approximate solutions are in reasonable alignment with the exact solution when $\alpha = 1$ and the solutions are continuously based on a fractional derivative. The graph in Figure 1 (b) represent the absolute errors of $\theta(t)$.

Example 5.2. Consider the following system:

$$\begin{cases} \mathcal{D}^\alpha \omega = \omega^2 - 4(\omega - 1) - \cos^2(t) - \sin(t), \\ \mathcal{D}^\alpha \Theta = \omega \Theta - 2\Theta - t^2 \cos(t) + 2t, \end{cases} \quad 0 \leq t \leq 1,$$

with conditions:

$$\begin{cases} \omega(0) = 3, \\ \Theta(1) = 1, \end{cases}$$

when $\alpha = 1$ the exact solution is:

$$\begin{cases} \omega(t) = \cos(t) + 2, \\ \Theta(t) = t^2. \end{cases}$$

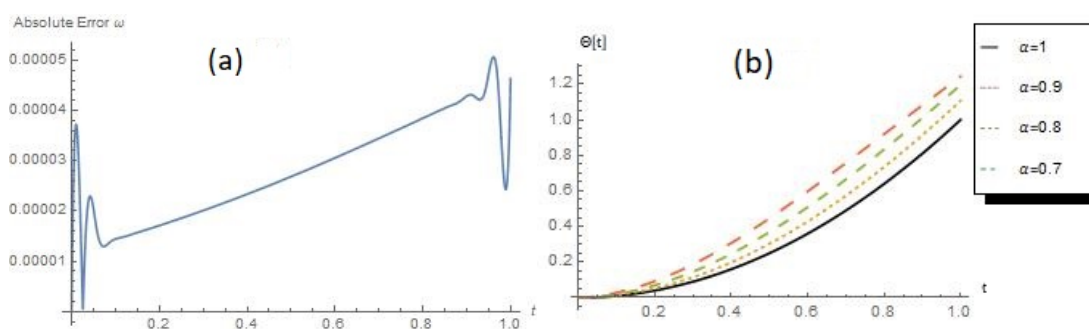
After homogenizing the initial conditions and using algorithm 1, apply $t_i = \frac{i}{n}$, $i = 1, n$ and $n = 35$, the tables 3 and 4 describe the exact solutions of $\omega(t)$ and $\Theta(t)$ and approximate solutions for different values of α .

Table 3. Numerical results for $\omega(t)$ of example 5.2.

t	Exact Sol of $\omega(t)$	App Sol of $\omega(t)$	$\alpha = 0.9$	$\alpha = 0.8$	$\alpha = 0.7$	Abs Error
0.	3.	3.	3.	3.	3.	0.
0.2	2.98007	2.98008	2.97308	2.96301	2.94782	$1.71231717 \times 10^{-5}$
0.4	2.92106	2.92108	2.89745	2.86363	2.81286	$2.336775593 \times 10^{-5}$
0.6	2.82534	2.82537	2.77748	2.71004	2.61271	$3.05778094 \times 10^{-5}$
0.8	2.69671	2.69675	2.6203	2.51736	2.38161	$3.84719926 \times 10^{-5}$
1.	2.5403	2.54035	2.43686	2.3082	2.15981	$4.636294967 \times 10^{-5}$

Table 4. Numerical results for $\Theta(t)$ of example 5.2.

t	Exact Sol of $\Theta(t)$	App Sol of $\Theta(t)$	$\alpha = 0.9$	$\alpha = 0.8$	$\alpha = 0.7$	Abs Error
0.	0.	0.	0.	0.	0.	0.
0.2	0.04	0.0399862	0.0526074	0.0695245	0.0925163	$1.379651819 \times 10^{-5}$
0.4	0.16	0.159985	0.198264	0.246476	0.306978	$1.465169064 \times 10^{-5}$
0.6	0.36	0.359987	0.428814	0.509138	0.597815	$1.348748932 \times 10^{-5}$
0.8	0.64	0.639991	0.735269	0.833398	0.919358	$9.089432173 \times 10^{-6}$
1.	1.	1.	1.10687	1.19567	1.24369	0.

**Figure 2.** Solution and graphical curves of Example 5.2.

Graphs of the approximate solutions of $\theta(t)$ are plotted in Figure 2 (b) for different values of α . The graph in Figure 2 (a) represent the absolute errors of $\omega(t)$.

Example 5.3. Consider the following fractional system:

$$\begin{cases} \mathcal{D}^\alpha \omega = \Theta - \rho + t, \\ \mathcal{D}^\alpha \Theta = 3t^2, \\ \mathcal{D}^\alpha \rho = \Theta + e^{-t}, \quad 0 \leq t \leq 1, \end{cases}$$

subject to:

$$\begin{cases} \omega(0) = 1, \\ \Theta(0) = 1, \\ \rho(1) = 1.25 - e^{-1}, \end{cases}$$

with exact solution:

$$\begin{cases} \omega(t) = -0.05t^5 + 0.25t^4 + t + 2 - e^{-t}, \\ \Theta(t) = t^3 + 1, \\ \rho(t) = 0.25t^4 + t - e^{-t}. \end{cases}$$

After the initial conditions have been homogenised and algorithm 1 used, apply $t_i = \frac{i}{n}$, $i = 1, n$ and $n = 30$, the tables 5–7 describe the exact solutions of $\omega(t)$, $\Theta(t)$ and ρ and approximate solutions for different values of α .

Table 5. Numerical results for $\omega(t)$ of example 5.3.

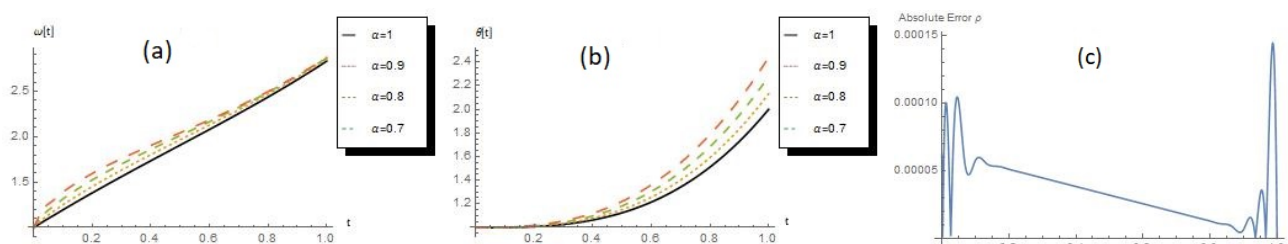
t	Exact Sol of $\omega(t)$	App Sol of $\omega(t)$	$\alpha = 0.9$	$\alpha = 0.8$	$\alpha = 0.7$	Absolute Error
0.	1.	1.	1.	1.	1.	0.
0.2	1.38165	1.38163	1.45132	1.52412	1.59527	$2.778531454 \times 10^{-5}$
0.4	1.73557	1.73552	1.80231	1.85993	1.90359	$4.434730105 \times 10^{-5}$
0.6	2.0797	2.07964	2.12935	2.16496	2.18472	$5.613341879 \times 10^{-5}$
0.8	2.43669	2.43662	2.46954	2.48922	2.49658	$6.305905268 \times 10^{-5}$
1.	2.83212	2.83206	2.8543	2.86685	2.87146	$6.508054219 \times 10^{-5}$

Table 6. Numerical results for $\Theta(t)$ of example 5.3.

t	Exact Sol of $\Theta(t)$	App Sol of $\Theta(t)$	$\alpha = 0.9$	$\alpha = 0.8$	$\alpha = 0.7$	Absolute Error
0.	1.	1.	1.	1.	1.	0.
0.2	1.008	1.38163	1.01064	1.01411	1.01865	$7.327471963 \times 10^{-15}$
0.4	1.064	1.73552	1.07942	1.09826	1.1212	$1.720845688 \times 10^{-13}$
0.6	1.216	2.07964	1.25738	1.30578	1.36221	$8.968381593 \times 10^{-13}$
0.8	1.512	2.43662	1.59278	1.6843	1.78757	$1.98951966 \times 10^{-12}$
1.	2.	2.83206	2.13222	2.27818	2.43862	$1.869615573 \times 10^{-12}$

Table 7. Numerical results for $\rho(t)$ of example 5.3.

t	Exact Sol of $\rho(t)$	App Sol of $\rho(t)$	$\alpha = 0.9$	$\alpha = 0.8$	$\alpha = 0.7$	Absolute Error
0.	-1.	-1.	-1.	-1.	-1.	0.
0.2	-0.618331	-0.61828	-0.534717	-0.436751	-0.323107	$5.101539186 \times 10^{-5}$
0.4	-0.26392	-0.263882	-0.161995	-0.0516111	0.0670132	$3.825972939 \times 10^{-5}$
0.6	0.0835884	0.0836139	0.191075	0.304226	0.423533	$2.55064838 \times 10^{-5}$
0.8	0.453071	0.453084	0.568489	0.69138	0.823913	$1.275324046 \times 10^{-5}$
1.	0.882121	0.882121	1.01733	1.16604	1.3321	0.

**Figure 3.** Solution and graphical curves of Example 5.3.

Graphs of the approximate solutions of $\omega(t)$ and $\theta(t)$ are plotted in Figure 3 (a), Figure 3 (b) for different values of α . The graph in Figure 3 (c) represent the absolute errors of $\rho(t)$.

Now, we consider the following tables where the RKHS method has been applied in order to give numerical approximations with other values of n , and then compare it with finite difference and collocation methods.

Table 8. Error in $\omega(t)$ of the first example.

t	Error in $\omega(t)$ by RKHS for n=40	Error in $\omega(t)$ by RKHS for n=100	Error in $\omega(t)$ by Finite difference	Error in $\omega(t)$ by Collocation
0	0.	Indeterminate	0.	0.
0.1	2.89×10^{-5}	3.93×10^{-6}	2.08×10^{-2}	1.62×10^{-4}
0.2	1.69×10^{-5}	1.65×10^{-6}	3.25×10^{-2}	8.06×10^{-4}
0.3	7.64×10^{-6}	8.48×10^{-7}	3.79×10^{-2}	4.04×10^{-4}
0.4	5.45×10^{-7}	4.29×10^{-9}	3.89×10^{-2}	1.61×10^{-4}
0.5	4.84×10^{-6}	4.19×10^{-7}	3.70×10^{-2}	1.73×10^{-4}

Table 9. Error in $\Theta(t)$ of the first example.

t	Error in $\Theta(t)$ by RKHS for n=40	Error in $\Theta(t)$ by RKHS for n=100	Error in $\Theta(t)$ by Finite difference	Error in $\Theta(t)$ by Collocation
0	0.	Indeterminate	2.81×10^{-2}	1.41×10^{-4}
0.1	1.71×10^{-6}	4.40×10^{-6}	1.40×10^{-2}	2.77×10^{-5}
0.2	5.63×10^{-6}	1.86×10^{-6}	5.01×10^{-3}	7.64×10^{-5}
0.3	1.11×10^{-5}	8.21×10^{-7}	7.39×10^{-4}	9.81×10^{-5}
0.4	1.52×10^{-5}	9.84×10^{-7}	6.04×10^{-4}	1.31×10^{-4}
0.5	1.82×10^{-5}	1.14×10^{-6}	0.	0.

Table 10. Error in $\omega(t)$ of the second example.

t	Error in $\omega(t)$ by RKHS for n=35	Error in $\omega(t)$ by RKHS for n=60	Error in $\omega(t)$ by RKHS for n=100	Error in $\omega(t)$ by Finite difference	Error in $\omega(t)$ by Collocation
0	0.	0.	0.	0.	Failed
0.2	1.71×10^{-5}	3.44×10^{-6}	2.51×10^{-7}	1.09×10^{-2}	Failed
0.4	2.33×10^{-5}	4.69×10^{-6}	3.49×10^{-7}	2.62×10^{-2}	Failed
0.6	3.05×10^{-5}	6.14×10^{-6}	4.73×10^{-7}	4.63×10^{-2}	Failed
0.8	3.84×10^{-5}	7.73×10^{-6}	5.98×10^{-7}	7.11×10^{-2}	Failed
1	4.63×10^{-5}	9.73×10^{-6}	7.45×10^{-7}	9.91×10^{-2}	Failed

Table 11. Error in $\Theta(t)$ of the second example.

t	Error in $\Theta(t)$ by RKHS for n=35	Error in $\Theta(t)$ by RKHS for n=60	Error in $\Theta(t)$ by RKHS for n=100	Error in $\Theta(t)$ by Finite difference	Error in $\Theta(t)$ by Collocation
0	0.	0.	0.	5.54×10^{-2}	Failed
0.2	1.37×10^{-5}	2.82×10^{-6}	2.51×10^{-7}	4.49×10^{-2}	Failed
0.4	1.46×10^{-5}	3.00×10^{-6}	3.49×10^{-7}	3.34×10^{-2}	Failed
0.6	1.34×10^{-5}	2.79×10^{-6}	4.73×10^{-7}	2.04×10^{-2}	Failed
0.8	9.08×10^{-6}	2.03×10^{-6}	5.98×10^{-7}	7.77×10^{-3}	Failed
1	0.	0.	0.	0.	Failed

Table 12. Error in $\omega(t)$ of the third example.

t	Error in $\omega(t)$ by RKHS for n=30	Error in $\omega(t)$ by RKHS for n=60	Error in $\omega(t)$ by Finite difference	Error in $\omega(t)$ by Collocation
0	0.	0.	0.	0.
0.2	2.77×10^{-5}	1.43×10^{-6}	2.83×10^{-3}	5.86×10^{-4}
0.4	4.43×10^{-5}	1.42×10^{-6}	1.24×10^{-2}	5.29×10^{-4}
0.6	5.61×10^{-5}	1.12×10^{-6}	3.13×10^{-2}	5.44×10^{-4}
0.8	6.30×10^{-5}	6.62×10^{-6}	6.06×10^{-2}	4.86×10^{-4}
1	6.50×10^{-5}	9.69×10^{-6}	1.00×10^{-2}	1.08×10^{-3}

Table 13. Error in $\Theta(t)$ of the third example.

t	Error in $\Theta(t)$ by RKHS for n=30	Error in $\Theta(t)$ by RKHS for n=60	Error in $\Theta(t)$ by Finite difference	Error in $\Theta(t)$ by Collocation
0	0.	0.	0.	0.
0.2	7.32×10^{-15}	6.28×10^{-13}	5.00×10^{-3}	0.
0.4	1.72×10^{-13}	2.80×10^{-13}	2.20×10^{-2}	0.
0.6	8.96×10^{-13}	4.10×10^{-13}	5.10×10^{-2}	0.
0.8	1.98×10^{-12}	5.94×10^{-13}	9.20×10^{-2}	0.
1	1.86×10^{-12}	5.37×10^{-14}	1.45×10^{-1}	0.

Table 14. Error in $\rho(t)$ of the third example.

t	Error in $\rho(t)$ by RKHS for n=30	Error in $\rho(t)$ by RKHS for n=60	Error in $\rho(t)$ by Finite difference	Error in $\rho(t)$ by Collocation
0	0.	0.	5.59×10^{-2}	1.29×10^{-4}
0.2	5.10×10^{-5}	1.48×10^{-6}	6.47×10^{-2}	5.49×10^{-5}
0.4	3.82×10^{-5}	3.07×10^{-6}	6.80×10^{-2}	6.03×10^{-5}
0.6	2.55×10^{-5}	4.66×10^{-6}	6.14×10^{-2}	5.73×10^{-5}
0.8	1.27×10^{-5}	6.26×10^{-6}	4.03×10^{-2}	6.23×10^{-5}
1	0.	0.	0.	0.

6. Conclusions

In this article, we effectively utilize the RKHSM to develop an approximate solution of differential fractional equations with temporal two-point BVP. The results of examples demonstrate reliability and consistency of the method. In the future, we recommend further research on the RKHS method, as solving the temporal two-point boundary value problems with the conformable and the Atangana-Baleanu derivatives. We expect to achieve better results and good approximations for the solutions.

Conflict of interest

The authors state that they have no conflict of interest. All authors have worked in an equal sense to find these results.

References

1. C. Li, D. Qian, Y. Chen, On Riemann-Liouville and Caputo derivatives, *Discrete Dyn. Nat. Soc.*, **2011** (2011), 1–15.
2. R. Hilfer, Y. Luchko, Z. Tomovski, Operational method for the solution of fractional differential equations with generalized Riemann-Liouville fractional derivatives, *Fract. Calc. Appl. Anal.*, **12** (2009), 299–318.
3. M. D. Ortigueira, L. Rodríguez-Germá, J. J. Trujillo, Complex Grünwald-Letnikov, Liouville, Riemann-Liouville, and Caputo derivatives for analytic functions, *Commun. Nonlinear Sci.*, **16** (2011), 4174–4182.
4. R. Khalil, M. Al Horani, A. Yousef, M. Sababheh, A new definition of fractional derivative, *J. Comput. Appl. Math.*, **264** (2014), 65–70.
5. O. A. Arqub, B. Maayah, Modulation of reproducing kernel Hilbert space method for numerical solutions of Riccati and Bernoulli equations in the Atangana-Baleanu fractional sense, *Chaos Soliton. Fract.*, **125** (2019), 163–170.
6. J. Cresson, P. Inizan, Variational formulations of differential equations and asymmetric fractional embedding, *J. Math. Anal. Appl.*, **385** (2012), 975–997.
7. G. Jumarie, Table of some basic fractional calculus formulae derived from a modified Riemann-Liouville derivative for non-differentiable functions, *Appl. Math. Lett.*, **22** (2009), 378–385.
8. B. S. H. Kashkari, M. I. Syam, Reproducing Kernel Method for Solving Nonlinear Fractional Fredholm Integro-differential Equation, *Complexity*, **2018** (2018), 1–7.
9. O. A. Arqub, B. Maayah, Solutions of Bagley–Torvik and Painlevé equations of fractional order using iterative reproducing kernel algorithm with error estimates, *Neural Comput. Appl.*, **29** (2018), 1465–1479.
10. A. K. Albzeirat, M. Z. Ahmad, S. M. Momani, B. Maayah, Numerical solution of second-order fuzzy differential equation of integer and fractional order using reproducing kernel Hilbert space method tools, *Far East Journal of Mathematical Sciences*, **101** (2017), 1327–1351.
11. Y. Ren, Y. Qin, R. Sakthivel, Existence results for fractional order semilinear integro-differential evolution equations with infinite delay, *Integr. Equat. Oper. Th.*, **67** (2010), 33–49.
12. L. Xu, X. Chu, H. Hu, Exponential ultimate boundedness of non-autonomous fractional differential systems with time delay and impulses, *Appl. Math. Lett.*, **99** (2020), 106000.
13. L. Xu, H. Hu, F. Qin, Ultimate boundedness of impulsive fractional differential equations, *Appl. Math. Lett.*, **62** (2016), 110–117.
14. X. Chu, L. Xu, H. Hu, Exponential quasi-synchronization of conformable fractional-order complex dynamical networks, *Chaos Soliton. Fract.*, **144** (2020), 110268.
15. A. Berlinet, C. Thomas-Agnan, *Reproducing Kernel Hilbert Spaces in Probability and Statistics*, Springer US, 2004.
16. B. Sriperumbudur, A. Gretton, K. Fukumizu, Hilbert space embeddings and metrics on probability measures, *J. Mach. Learn. Res.*, **11** (2010), 1517–1561.

17. R. Magin, Fractional calculus models of complex dynamics in biological tissues, *Comput. Math. Appl.*, **59** (2010), 1586–1593.
18. R. Almeida, A. B. Malinowska, A fractional calculus of variations for multiple integrals with application to vibrating string, *J. Math. Phys.*, **51** (2010), 1–12.
19. J. Lin, L. Rosasco, Generalization properties of doubly stochastic learning algorithms, *J. Complexity*, **47** (2018), 42–61.
20. O. A. Arqub, B. Maayah, Numerical solutions of integrodifferential equations of Fredholm operator type in the sense of the Atangana–Baleanu fractional operator, *Chaos Soliton. Fract.*, **117** (2018), 117–124.
21. O. A. Arqub, Fitted reproducing kernel Hilbert space method for the solutions of some certain classes of time-fractional partial differential equations subject to initial and Neumann boundary conditions, *Appl. Math. Comput.*, **73** (2007), 1243–1261.
22. M. Klimek, Stationarity-conservation laws for fractional differential equations with variable coefficients, *J. Phys. A-Math. Gen.*, **35** (2002), 6675–6693.
23. H. Beyrami, T. Lotfi, K. Mahdiani, Stability and error analysis of the reproducing kernel Hilbert space method for the solution of weakly singular Volterra integral equation on graded mesh, *Appl. Numer. Math.*, **120** (2017), 197–214.
24. S. Javan, S. Abbasbandy, M. Araghi, Application of Reproducing Kernel Hilbert Space Method for Solving a Class of Nonlinear Integral Equations, *Math. Probl. Eng.*, **2017** (2017), 1–10.
25. O. A. Arqub, M. Al-Smadi, N. Shawagfeh, Solving Fredholm integrodifferential equations using reproducing kernel Hilbert space method, *Appl. Math. Comput.*, **219** (2013), 8938–8948.
26. M. Al-Smadi, O. A. Arqub, S. Momani, A computational method for two-point boundary value problems of fourth-order mixed integrodifferential equations, *Math. Probl. Eng.*, **2013** (2013), 1–10.
27. S. Bushnaq, B. Maayah, M. Ahmad, Reproducing kernel Hilbert space method for solving fredholm integrodifferential equations of fractional order, *Italian Journal of Pure and Applied Mathematics*, **36** (2016), 307–318.
28. A. AlHabees, B. Maayah, S. Bushnaq, Solving fractional proportional delay integrodifferential equations of first order by reproducing kernel Hilbert space method, *Global Journal of Pure and Applied Mathematics*, **12** (2016), 3499–3516.
29. S. Bushnaq, B. Maayah, S. Momani, A. Alsaedi, A reproducing kernel Hilbert space method for solving systems of fractional integrodifferential equations, *Abstr. Appl. Anal.*, **2014** (2014), 1–6.
30. Z. Altawallbeh, M. Al-Smadi, R. Abu-Gdairi, Approximate solution of second-order integrodifferential equation of Volterra type in RKHS method, *Int. Journal of Math. Analysis*, **7** (2013), 2145–2160.
31. B. Maayah, S. Bushnaq, M. Ahmad, S. Momani, Computational method for solving nonlinear voltera integro-differential equations, *J. Comput. Theor. Nanos.*, **13** (2016), 7802–7806.
32. O. A. Arqub, Reproducing kernel algorithm for the analytical-numerical solutions of nonlinear systems of singular periodic boundary value problems, *Math. Probl. Eng.*, **2015** (2015), 1–13.

33. Z. Altawallbeh, M. Al-Smadi, I. Komashynska, A. Atewi, Numerical Solutions of Fractional Systems of Two-Point BVPs by Using the Iterative Reproducing Kernel Algorithm, *Ukrainian Mathematical Journal*, **70** (2018), 687–701.
34. S. Bushnaq, B. Maayah, A. AlHabees, Application of multistep reproducing kernel Hilbert space method for solving giving up smoking model, *International Journal of Pure and Applied Mathematics*, **109** (2016), 311–324.
35. M. Inc, A. Akgül, The reproducing kernel Hilbert space method for solving Troesch's problem, *Journal of the Association of Arab Universities for Basic and Applied Sciences*, **14** (2013), 19–27.
36. Z. Zhao, Y. Lin, J. Niu, Convergence Order of the Reproducing Kernel Method for Solving Boundary Value Problems, *Math. Model. Anal.*, **21** (2016), 466–477.
37. X. Lù, M. Cui, Existence and numerical method for nonlinear third-order boundary value problem in the reproducing kernel space, *Bound. Value Probl.*, **2010** (2010), 1–19.
38. B. Maayah, S. Bushnaq, A. Alsaedi, S. Momani, An efficient numerical method for solving chaotic and non-chaotic systems, *J. Ramanujan Math. Soc.*, **33** (2018), 219–231.
39. B. Maayah, S. Bushnaq, S. Momani, O. A. Arqub, Iterative multistep reproducing kernel Hilbert space method for solving strongly nonlinear oscillators, *Adv. Math. Phys.*, **2014** (2014), 1–7.
40. M. Al-Smadi, A. Freihat, H. Khalil, Numerical Multistep Approach for Solving Fractional Partial Differential Equations, *Int. J. Comput. Meth.*, **14** (2017), 1–15.
41. S. Bushnaq, B. Maayah, S. M. Momani, O. A. Arqub, Analytical simulation of singular second-order, three points boundary value problems for fredholm operator using computational kernel algorithm, *J. Comput. Theor. Nanos.*, **13** (2016), 7816–7824.
42. K. Moaddy, A. Freihat, M. Al-Smadi, E. Abuteen, I. Hashim, Numerical investigation for handling fractional-order Rabinovich–Fabrikant model using the multistep approach, *Soft Comput.*, **22** (2018), 773–782.
43. D. Morrison, J. Riley, J. Zancanaro, Multiple shooting method for two-point boundary value problems, *Commun. ACM*, **5** (1962), 613–614.
44. S. Filipov, I. Gospodinov, I. Faragó, Shooting-projection method for two-point boundary value problems, *Appl. Math. Lett.*, **72** (2017), 10–15.
45. R. Russell, L. Shampine, A collocation method for boundary value problems, *Numer. Math.*, **19** (1972), 1–28.
46. H. Liang, M. Stynes, Collocation Methods for General Caputo Two-Point Boundary Value Problems, *J. Sci. Comput.*, **76** (2018), 390–425.
47. R. P. Agarwal, Y. M. Chow, Finite-difference methods for boundary-value problems of differential equations with deviating arguments, *Comput. Math. Appl.*, **12** (1986), 1143–1153.
48. M. M. Chawla, C. P. Katti, Finite difference methods for two-point boundary value problems involving high order differential equations, *BIT Numerical Mathematics*, **19** (1979), 27–33.
49. A. Miele, R. Iyer, Modified quasilinearization method for solving nonlinear, two-point boundary-value problems, *J. Math. Anal. Appl.*, **36** (1971), 674–692.

50. R. Sylvester, F. Meyer, Two Point Boundary Problems by Quasilinearization, *Journal of the Society for Industrial and Applied Mathematics*, **13** (1965), 586–602.
51. O. A. Arqub, Z. Abo-Hammour, S. Momani, N. Shawagfeh, Solving singular two-point boundary value problems using continuous genetic algorithm, *Abstr. Appl. Anal.*, **2012** (2012), 1–25.
52. Z. Abo-Hammour, M. Yusuf, N. Mirza, S. Mirza, Numerical solution of second-order, two-point boundary value problems using continuous genetic algorithms, *Int. J. Numer. Meth. Eng.*, **61** (2004), 1219–1242.
53. H. Jaradat, *Numerical solution of temporal two-point boundary value problems using continuous genetic algorithms*, University of Jordan, 2006.
54. I. Podlubny, *Fractional differential equations: An introduction to fractional derivatives, fractional differential equations, to methods of their solution and some of their applications*, Academic Press, 1998.
55. K. Diethelm, *The analysis of fractional differential equations*, Springer Verlag, Berlin, Heidelberg, 2010.
56. C. Li, M. Cui, The exact solution for solving a class nonlinear operator equations in the reproducing kernel space, *Appl. Math. Comput.*, **143** (2003), 393–399.
57. M. Cui, Y. Lin, *Nonlinear Numerical Analysis in Reproducing Kernel Space*, Nova Science Publishers, 2009.



AIMS Press

©2021 the Author(s), licensee AIMS Press. This is an open access article distributed under the terms of the Creative Commons Attribution License (<http://creativecommons.org/licenses/by/4.0>)